Article

Chinese Science Bulletin

Fluid Mechanics

May 2012 Vol.57 No.15: 1765–1771
doi: 10.1007/s11434-012-5124-0

Experimental investigation of supersonic flow over a hemisphere

WANG DengPan[1], ZHAO YuXin[1*], XIA ZhiXun[1], WANG QingHua[2] & HUANG LiYa[3]

[1] *Science and Technology on Scramjet Laboratory, National University of Defense Technology, Changsha 410073, China;*
[2] *The Third Institute, the Second Artillery Equipment Academy, Beijing 100085, China;*
[3] *College of Aerospace and Materials Engineering, National University of Defense Technology, Changsha 410073, China*

Received December 26, 2011; accepted March 5, 2012

The experimental investigation of supersonic flow over a hemisphere was conducted using Nanoparticle-based Planar Laser Scattering (NPLS) technique in a supersonic quiet wind tunnel at *Ma*=2.68. Ahead of the hemisphere, boundary layer separation with the formation of a three-dimensional separated flow was observed, which was resulted from the interaction between the three-dimensional bow shock wave and the boundary layer. The complex flow structures of supersonic flow over the hemisphere were visualized. Based on the time correlation of NPLS images, time-space evolutionary characteristics of supersonic flow over the hemisphere were studied, and the evolutionary characteristics of the spanwise and streamwise large scale vortex structures were obtained, which have the features of periodicity and similar geometry.

NPLS, shock wave, supersonic flow over a hemisphere, flow visualization

Citation: Wang D P, Zhao Y X, Xia Z X, et al. Experimental investigation of supersonic flow over a hemisphere. Chin Sci Bull, 2012, 57: 1765–1771, doi: 10.1007/s11434-012-5124-0

The protuberance is mounted on the surface or flow channel of the supersonic or hypersonic vehicle and the local structure of the flow field will be changed. Currently, achieving flow control has been becoming a research hotspot of supersonic flow. The study of the supersonic plate boundary layer and its interaction with the hemisphere has broad application background and high scientific value. The mutual interference of the hemisphere and supersonic flow generates complex flow field structures, which contain the three-dimensional detached shock wave, the surface topological structure, the circulating region in the downstream, the reattached shock wave and the wake. The complex flow field structures show the characteristics of the supersonic flow over a protuberance on the surface. Therefore the hemisphere can be used as a typical model to study the mechanism of the supersonic flow over a protuberance on the surface, and is also used to verify some questions that are disputed at present, such as the interaction of the three-dimensional curved shock wave and the boundary layer, the effect of the lateral pressure gradient on the surface flow spectrums and the dynamic characteristics of the supersonic vortical structure.

Unfortunately, the influences of strong discontinuity and diffusion factors, such as compressibility, turbulence, large scale structure, shock waves and slip line, make it difficult to get the fine structure of supersonic flow over a hemisphere by means of high resolution numerical simulation and measurement. Hawthorne and Martin [1] studied the flow over a hemisphere on the flat plate by means of calculation method in 1955. Zhang [2] studied the interaction of the shock wave and boundary layer about the external flow and internal flow, and provided the photos of typical flow spectrums of different experimental models, including the photos of supersonic flow over a sphere. Some research institutions have studied the typical flow field structures of the supersonic flow over different models by means of experimental and numerical methods at home and abroad, and the models included the cylinder [3–13], the boss [5,6], the blunt fin [5,12], the wedge-shaped obstacle and sweptback step [13], and the cone [14,15], which were used to study

*Corresponding author (email: zyx_nudt@yahoo.com.cn)

the problems of the three-dimensional flow field structure, the interaction of the shock wave and the boundary layer, and boundary layer separation. Korkegi [16,17] and Sedney [18,19] surveyed and analyzed the experiments of supersonic flow over high and low protuberances. Panov and Shvets [20] analyzed the experimental data of the interaction of shock waves with a turbulent boundary layer, and gave an empirical relationship between the critical pressure of the shock wave induced separation of the boundary layer and the mach number of the incident flow.

In recent years, nanoparticle-based planar laser scattering (NPLS) which is used to measure the supersonic flow was developed at the National University of Defence Technology (NUDT). The experimental system (NPLS) has been used in the research of supersonic mixing layer [21–24], boundary layer [25], flow over aircrafts and the aero-optical [26,27], and the numerous experimental data was obtained and had made some progress in the fields. In this paper, based on the characteristics of high resolution flow visualization of the NPLS system and combined with numerical simulation technology, the fine structures and evolutionary characteristics of supersonic flow over a hemisphere were made a deep study.

1 Experimental

1.1 Supersonic quiet wind tunnel

The experiments were conducted in a supersonic quiet wind tunnel (KD-2) at the National University of Defense Technology (NUDT), at Ma=2.68, the total pressure of inflow is 1 atm, and the total temperature is 300 K. The wind tunnel was mainly composed of transition section, stability section, nozzle, test section and vacuum tank. The transition section is used to collect air from the ambient atmosphere, and the air is dried and rectified in the stability section. The inflow has lower velocity, better uniformity and lower turbulence. Air-breathing supersonic quiet wind tunnel has lower total pressure and smaller Reynolds number in experiment section than the blow-down wind tunnel, which is helpful to achieve the laminarization of nozzle. The nozzle and test section were integrated, and the optical windows are designed in the walls of test section. The dimensions of the test section are 200 mm×200 mm with the length of 400 mm. Figure 1 shows the setup and schematic of the supersonic quiet wind tunnel.

1.2 NPLS experiment technique

The NPLS experimental system is a new technique for flow visualization, which uses nanoparticles as the tracer particles, which was developed by Zhao et al. [28]. The schematic of NPLS experimental system is illustrated in Figure 2. Due to the high spatial and temporal resolutions and high signal-noise ratio (SNR), the NPLS can clearly show the fine vortical structure in turbulent boundary layer, and directly manifest the peripheral flow field structure around a hemisphere and its effect on turbulent boundary layer. The system is used in the paper which is similar to the NPLS system of Zhao et al.

The illumination is a double-pulsed Nd:YAG laser, with output wavelength 532 nm, pulse energy 350 mJ at 6 ns. The actual exposure time of the camera is the same as the laser pulse by utilizing a filtering instrument. The instantaneous structures of the supersonic flow field will be recorded. The imaging device we used is an IMPERX digital camera, equipped with a NIKON 105 mm lens. The maximum magnification is 1:1, and the resolution of the CCD is 4096×2600 pixels. Two frames will be captured through external trigger, and the captured image data will be real time transmission to a computer memory by the image acquisition board. The trigger signal is provided by a synchronous controller, and thus can keep synchronous with the pulse laser. Tracing flow with nanoparticles is the core of NPLS, and the KD-5 nanoparticles generator is used in this study. The calibration experiments proved that the average diameter of generated nanoparticles is about 45 nm, which has good flow-following ability. The changes in speed and density in flow field will directly influence the concentration of nanoparticles and thus cause the change of image grayscale.

A schema of the NPLS is shown in Figure 2. The computer controls the collaboration of every component and collects the experimental images. The computer software generates signals of synchronizer, which controls the collaboration of other components. The timing diagrams of

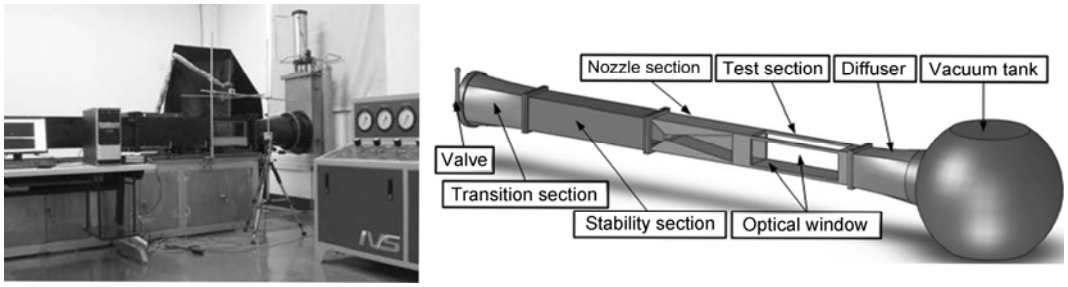

Figure 1 The setup and schematic of the supersonic quiet wind tunnel.

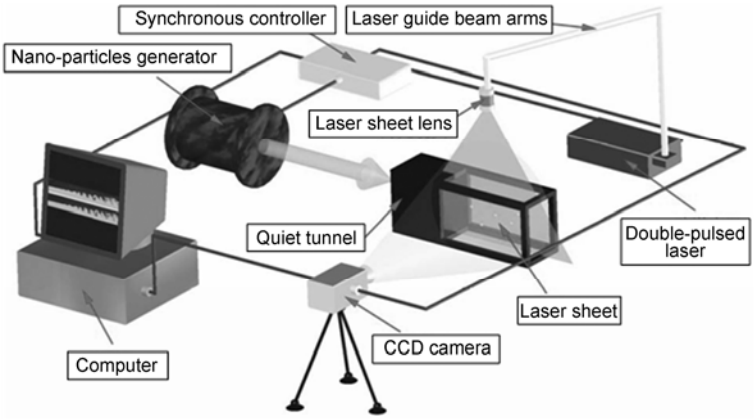

Figure 2 Schematic of NPLS experimental system.

exposure of CCD and laser output of pulse laser can be adjusted according to the purpose of measurement. The laser beam is transformed into a sheet with cylindrical lens. The nanoparticle generator is driven by high pressure N_2 gas, and the output particle concentration can be adjusted precisely by changing the pressure. While measuring a flow field with NPLS, the nanoparticles are injected into and mixed with the inflow of flow field. While the flow is established in the observing widow, the synchronizer controls the laser pulse and CCD to ensure synchronization of scattered laser by nanoparticles and the exposure of CCD.

1.3 Experimental model

The interactions of supersonic flow past a hemisphere were studied by mounting vertically the hemisphere on the symmetrical plane of a flat plate in the test section, and the flat plate is mounted on the braces, which is parallel to the direction of the inflow. The model of the test section and the coordinate system with respect to the hemisphere are shown in Figures 3 and 4, and the origin of coordinates is the centre of the hemisphere. The dimensions are as follow: 500 mm in length and 196 mm in width for the flat plate; radius of the hemisphere is R=10 mm, and the distance L is 132 mm from the centre of the hemisphere to the leading edge of the plate; R/δ=2.5, and δ represents the thickness of the supersonic flow boundary layer near the hemisphere.

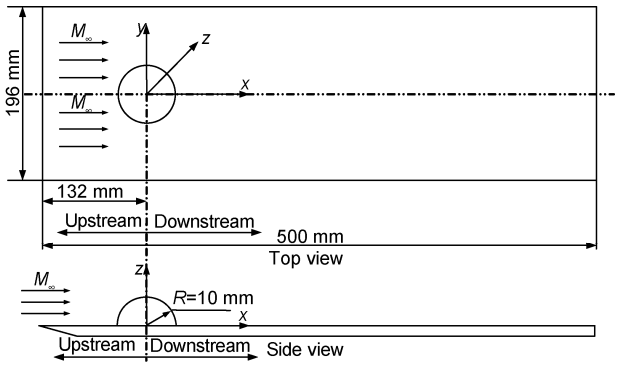

Figure 4 The coordinate system of the model.

To obtain the images of the interactions of supersonic flow past a hemisphere, the laser sheet is used to illuminate the flow and CCD camera is positioned vertical to the laser sheet. The laser sheet is positioned vertical to the plate and parallel to the incident flow. When we shoot the streamwise flow, the laser sheet is positioned horizontal to the plate and parallel to the incident flow, in order to shoot the spanwise flow. Schematics of shooting the flow field are shown in Figures 5 and 6.

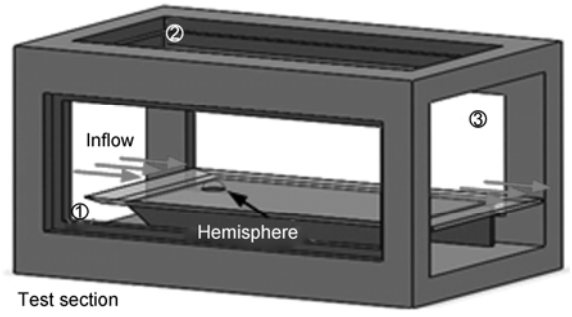

Figure 3 Schematic of the test section (①②③ represents the optical windows).

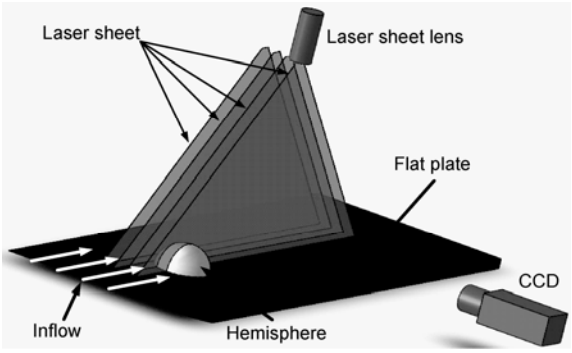

Figure 5 Schematics of shooting streamwise flow field.

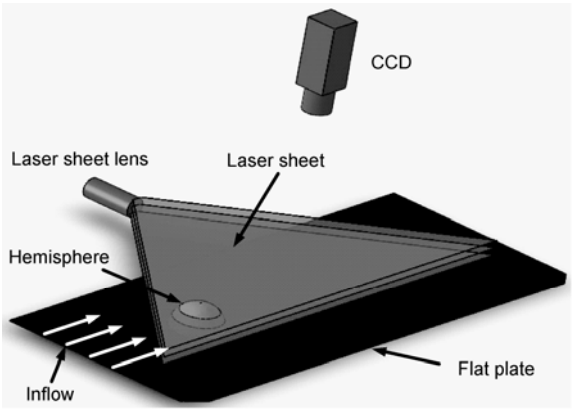

Figure 6 Schematics of shooting spanwise flow field.

2 The shock wave structures

Figure 7(a) and (b) show the NPLS images of supersonic flow over a hemisphere in the *x*-*y* and *x*-*z* planes with different positions of the laser sheet. Supersonic flowing over a hemisphere on the flat plate, a strong three-dimensional bow detached shock wave is observed, and as a result of the interaction of the shock wave and boundary layer, the three-dimensional bow boundary layer separated region is visualized ahead of the hemisphere as shown in Figure 7, marked by ⑥. In the supersonic flow field, there is a subsonic region in the boundary; however, the shock wave can be observed only in the region of supersonic, and it cannot extend to the plate through the boundary layer. This is shown clearly in Figure 7(a). The high pressure airflow behind the three-dimensional bow shock wave transfers upstream by the subsonic region in the bottom layer, and the strong adverse pressure gradient is formed in boundary layer. With the action of the adverse pressure gradient, the pressure of the upstream increases in the boundary layer which induces the laminar boundary layer thickening, transition and separation, and this induces a system of weak shock waves. The results are shown clearly in Figure 7(a), marked by ④.

Behind of the hemisphere, the complex trailing shock waves and a neck of wake are observed, as shown in Figure 7 and marked by ②, ③ and ⑤.

By contrasting and analyzing the NPLS images in the *x*-*z* and *x*-*y* plane, we know that the starting position of the reattachment shock wave is changing. The position of the laser sheet is changed from y=0 to y=10 mm, the height of starting position of the reattachment shock wave decreases gradually, and the distance in x direction increases at the beginning and then decreases, as shown in Figure 7 and marked by ②.

There are large-scale vortices generated behind the hemisphere, and the shocklets are induced whose intensity weaken and disappear while the vortexes move downstream, as shown in Figure 7 and marked by ②. Based on the NPLS images, the strong bow shock waves and expansion waves are formed near the hemisphere, which cause larger pressure-gradient, and with the interactions of streamwise velocity the trailing vortexes are induced. The airflow continuously sheds from the hemisphere, and is drawn continuously into the evolving streamwise vortexes. In the process of the continuous shedding and involution of vortexes, the low-speed flow is also drawn into the high-speed main stream, and forms streamwise vortexes whose velocity is lower than the velocity of main stream. Therefore, the local high-speed flow is blocked by the large scale vortex structures, and induces the evolving shocklets. As the flow moves downstream, the vortexes are accelerated by the high speed main stream, and the velocity of vortexes is gradually getting close to the velocity of main stream, which makes the comparative speed between the main stream and vortexes decrease. Therefore it is one of the reasons that the intensity of shocklets are weakened and disappeared.

3 The vortex structures

The NPLS images of supersonic flow over the hemisphere in the *x*-*y* and *x*-*z* plane are shown in Figure 8. The *x*-*y* images correspond to the flow field of the streamwise at the plane y=0, and the *x*-*z* images correspond to the flow field of the spanwise at the plane z=2 mm. The large scale turbulent coherent structures are observed behind the hemisphere. As shown in Figure 8, there are different zones of the grey scale in supersonic flow over the hemisphere. According to the basic principle of the NPLS, the lower of the airflow density and the lower of the nanoparticles concentration, the corresponding intensities of scattered light are weaker. There is a low density and pressure region behind the hemisphere which makes the grey scale lower.

Figure 8(a) shows that the large scale vortex structures in *x*-*z* plane behind the hemisphere have the geometric characteristics of periodicity and similarity. During the time interval of 15 μs, the displacement of the large scale vortices is obvious, and the changes of vortex structures are unobvious, which illustrates that the vortex structures in *x*-*z* plane have the characteristics of rapid transition and slow distortion along x direction. Based on the cross-correlation algorithm [29], the displacement of the large scale vortex structures increases gradually in x direction, 7.4 mm, 8.3 mm and 8.9 mm. From this we can judge, as a result of the exchange of energy, momentum and mass between the high-speed flow and bottom low-speed flow, the vortex structures are constantly accelerated in x direction.

Figure 8(b) shows that the vortex structures in *x*-*y* plane present obvious changes, but the evolutionary characteristics of the vortex structures can be identified, which illustrates that the large scale vortex structures in *x*-*y* plane have the geometric characteristics of periodicity and similarity.

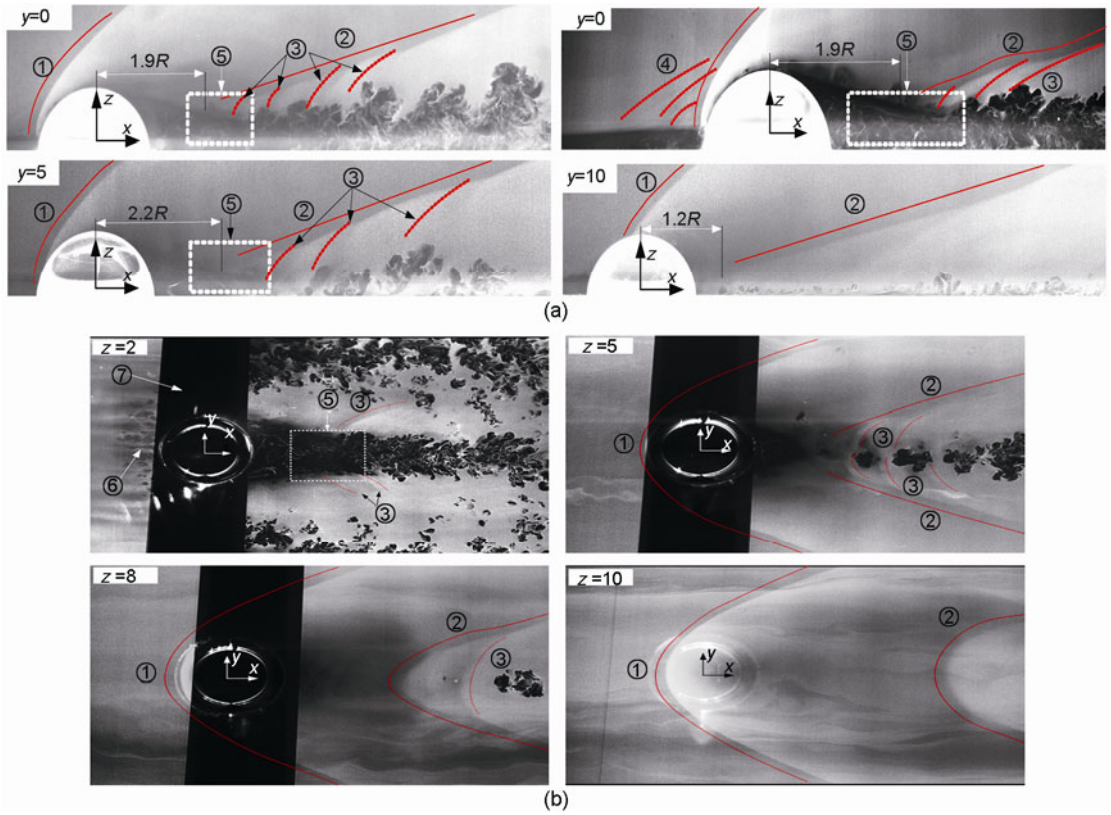

Figure 7 The NPLS images in the *x*-*y* and *x*-*z* planes with different positions of the laser sheet. (a) The images in the *x*-*z* plane with different positions of laser sheet (the laser sheet planes are as *y*=0, 5 and 10 mm); (b) the images in the *x*-*y* plane with different heights of laser sheet (the laser sheet planes are as *z*=2, 5, 8 and 10 mm). ① The three-dimensional bow detached shock wave; ② the reattachment shock wave behind the hemisphere; ③ shocklets; ④ a system of shock waves ahead of the hemisphere; ⑤ a neck of the wake; ⑥ the transition and separated region; ⑦ shade tape.

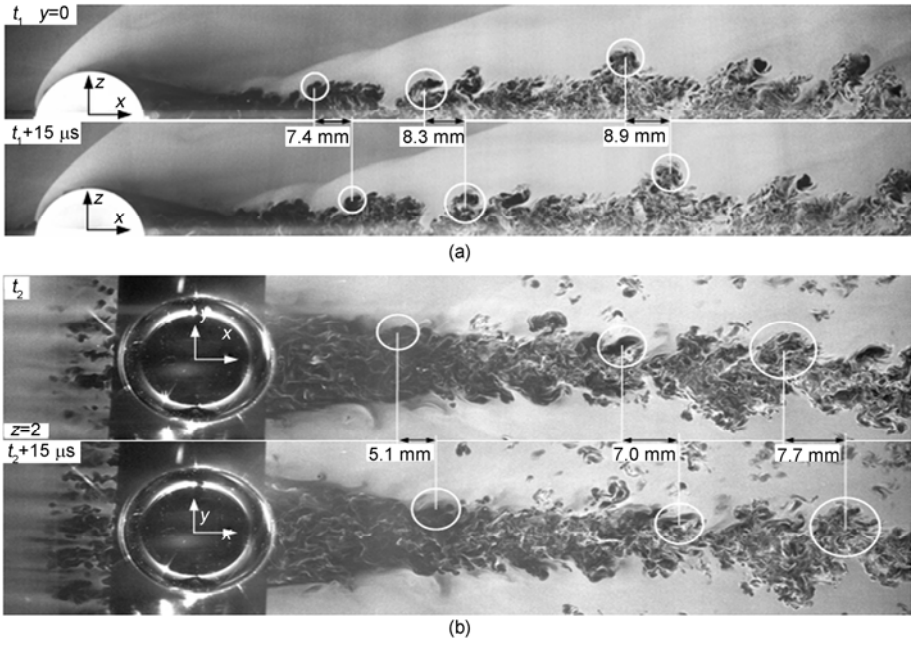

Figure 8 The NPLS images in *x*-*z* and *x*-*y* plane. (a) The NPLS images of the supersonic flow over the hemisphere at the plane *y*=0 (The stride frame time is 15 μs, the images' corresponding actual height and length of flow field are 23 mm and 190 mm, the spatial resolution is 0.0475 mm/pixel, and the distance from the left end of the images to the leading edge of the plate is 132 mm); (b) the NPLS images of the supersonic flow past a hemisphere at the plane *z*=2 mm (The stride frame time is 15 μs, the images' corresponding actual width and length of flow field are 30 mm and 120 mm, the spatial resolution is 0.03 mm/pixel, and the distance from the left end of the images to the leading edge of the plate is 132 mm).

Contrasting the vortex structures in *x*-*z* and *z*-*y* planes, we can know that the evolution of vortex structures in *x*-*y* plane is faster and more obvious than the changes in *x*-*z* plane, which indicates the characteristics of rapid moving and changing. Based on the cross-correlation algorithm, the similar results to the vortex structures in *x*-*z* plane were obtained, the displacement of the large scale vortex structures increases gradually in *x* direction, and the vortexes structures are constantly accelerated in *x* direction.

The NPLS images and the density contour in the *x*-*y* and *x*-*z* plane are shown in Figure 9. With the interaction between the three-dimensional bow shock wave and the supersonic laminar boundary layer, a separated region is formed in the boundary layer with the formation of an open three-dimensional separated region ahead of the hemisphere. The vortex structures in the separated region are strip shaped in the *x* direction, which are similar to the hairpin generated by the natural boundary layer transition. However, the vortex structures near the hemisphere evolve rapidly, which causes the time correlation of the two frames images bad, and it is difficult to determine the evolutionary characteristics of the vortex structures with the time correlation of the static NPLS images. However the evolutionary characteristics of the coherent vortexes structures can be observed by playing continuously two frames NPLS images. There is an expansion zone observed in the downstream of the recirculating region. In this paper, the flow field near the hemisphere is investigated numerically to observe further

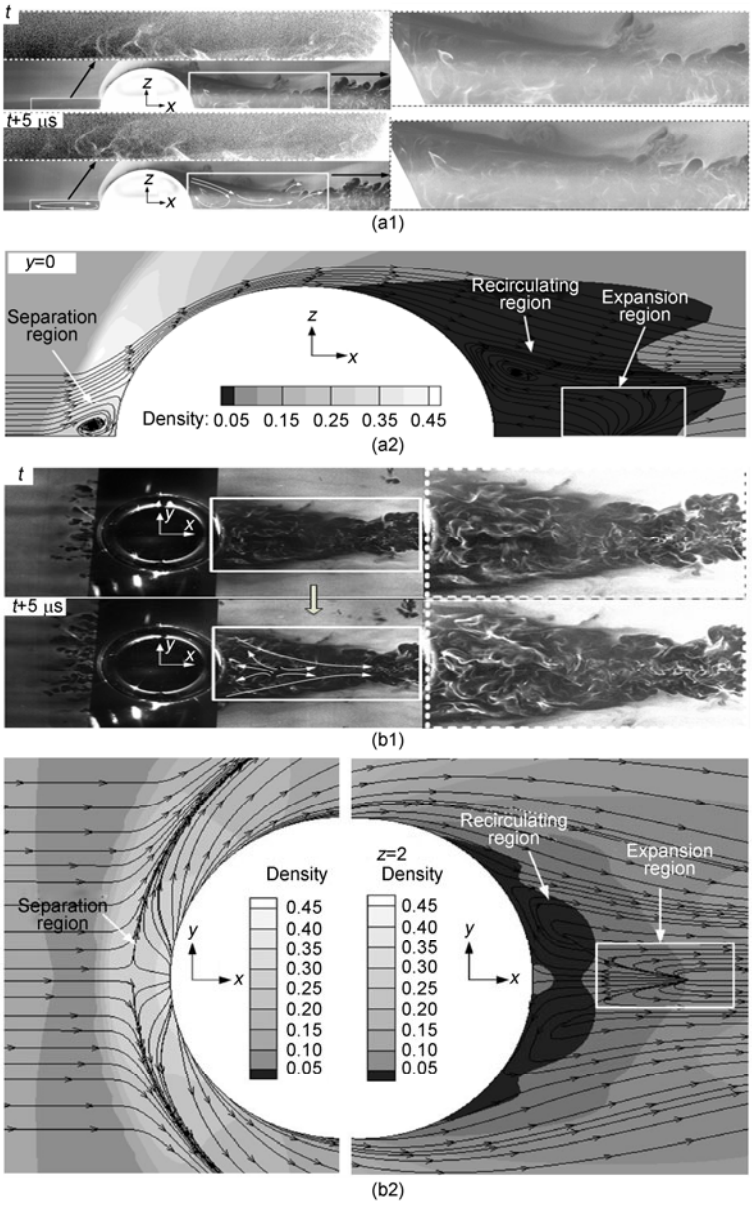

Figure 9 The *x*-*z* and *x*-*y* NPLS images, enlarged views and density contour near the hemisphere. (a) The *x*-*z* NPLS images, enlarged view and density contour near the hemisphere at *y*=0; (b) the *x*-*y* NPLS images, enlarged view at *z*=2 mm and density contour at *z*=0.1 and 2.

the features of the flow. Figure 9(a2) and (b2) are the numerical results. According to the streamline direction, we can know that there is a separation region and a recirculating region with a rotation in clockwise direction generated in the upstream and downstream of the hemisphere respectively, and an expansion zone is also observed near the recirculating region, which is similar to the fountain.

Based on the results of the NPLS images and numerical study, in supersonic flow over the hemisphere on the flat plate, there is a separation region and a recirculating region with a rotation in clockwise direction generated in the upstream and downstream of the hemisphere respectively, and an expansion zone is observed near the recirculating region where the airflow moves outward and perpendicularly to the paper, one of the causes of which is the evolution of the three-dimensional vortex structures.

4 Conclusions

In this paper, using the technique of high resolution flow visualization which was developed recently, the high spatiotemporal resolution images of supersonic laminar flow over the hemisphere were obtained. The analyzed results indicate that the structures of supersonic laminar flow over the hemisphere are very complex, especially which have extremely complex characteristics of the spatial structure and time evolution in the fields of the interaction between the three-dimensional detached shock wave and the boundary layer, the circulating region in the downstream and the shock wave induced by the wake. The results indicated that the strong three-dimensional detached bow shock wave generates in the upstream, and the interaction between shock wave and boundary layer causes the three-dimensional high pressure zone to move upriver which induces the laminar boundary layer instability and generates striped the structure of three-dimensional separations. At the downstream, a three-dimensional reattachment shock wave and the shocklets are observed, and a recirculating region with clockwise direction of rotation is formed. In the wake region, the large scale vortex structures show the characteristics of the periodicity and geometric similarity.

This work was supported by the National Natural Science Foundation of China (11072264).

1 Hawthorne W R, Martin M E. The effect of density gradient and shear on the flow over a hemisphere. Proc R Soc Lond A, 1955, 232: 184–195
2 Zhang Y. Expansion Wave and Shock Wave (in Chinese). Beijing: Peking University Press, 1983
3 Voitenko D M, Zubkov A I, Panov Y A. Supersonrc gas flow past a cylindrical obstacle on a plate. Fluid Dyn, 1966, 1: 121–125
4 Özcan O, Holt M. Supersonic separated flow past a cylindrical obstacle on a flat plate. AIAA J, 1984, 22: 611–617
5 Li S X. Complex Flow with the Leading of Shock Wave and Boundary Layer (in Chinese). Beijing: Science Press, 2007
6 Settles G S, Teng H Y. Cylindrical and conical flow regimes of three-dimensional shock/boundary-layer interactions. AIAA J, 1984, 22: 194–200
7 Bashkin V A, Egorov I V, Egorova M V. Supersonic viscous perfect gas flow past a circular cylinder. Fluid Dyn, 1993, 28: 833–838
8 Bashkin V A, Egorov I V, Egorova M V, et al. Supersonic laminar-turbulent gas flow past a circular cylinder. Fluid Dyn, 2000, 35: 652–662
9 Bashkin V A, Egorov I V, Egorova M V, et al. Supersonic flow past a circular cylinder with an isothermal surface. Fluid Dyn, 2001, 36: 147–153
10 Bashkin V A, Vaganov A V, Egorov I V, et al. Comparison of calculated and experimental data on supersonic flow past a circular cylinder. Fluid Dyn, 2002, 37: 473–483
11 Xu C Y, Chen L W, Lu X Y. Effect of Mach number on transonic flow past a circular cylinder. Chin Sci Bull, 2009, 54: 1886–1893
12 Dolling D S, Bogdonoff S M. Blunt fin-induced shock wave/turbulent boundary-layer interaction. AIAA J, 1982, 20: 1674–1680
13 Zheltovodov A A. Properties of two- and three-dimensional separation flows at supersonic velocities. Fluid Dyn, 1979, 14: 357–364
14 Avduevskii V S, Medvedev K I. Study of laminar boundary layer separation on a cone at an angle of attack. Fluid Dyn, 1966, 1: 78–80
15 Avduevskii V S, Medvedev K I. Separation of a three-dimensional boundary layer. Fluid Dyn, 1966, 1: 11–15
16 Korkegi R H. Survey of viscous interactions associated with high Mach number flight. AIAA J, 1971, 9: 771–784
17 Korkegi R H. Effect of transition on three-dimensional shock wave/boundary-layer interaction. AIAA J, 1972, 10: 361–363
18 Sedney R. A survey of the effects of small protuberances on boundary-layer flows. AIAA J, 1973, 11: 782–792
19 Sedney R, Kitchens C W Jr. Separation ahead of protuberances in supersonic turbulent boundary layers. AIAA J, 1977, 15: 546–552
20 Panov Yu A, Shvets A I. Separation of a turbulent boundary layer in a supersonic flow. Prikladnaya Mekhanika, 1966, 2: 99–105
21 Zhao Y X. Experimental investigation of spatiotemporal structures of supersonic mixing layer (in Chinese). Ph.D. Thesis. Changsha: National University of Defense Technology, 2008
22 Zhao Y X, Yi S H, He L. The fractal measurement of experimental images of supersonic turbulent mixing layer. Sci China Ser G-Phys Mech Astron, 2008, 52: 1134–1143
23 Yi S H, He L, Zhao Y X. A flow control study of a supersonic mixing layer via NPLS. Sci China Ser G-Phys Mech Astron, 2009, 52: 2001–2006
24 Zhao Y X, Yi S H, Tian L F. Multiresolution analysis of density fluctuation in supersonic mixing layer. Sci China Tech Sci, 2010, 53: 584–591
25 He L, Yi S H, Zhao Y X. Visualization of coherent structures in a supersonic flat-plate boundary layer. Chin Sci Bull, 2011, 56: 489–494
26 Yi S H, Tian L F, Zhao Y X. Aero-optical aberration measuring method based on NPLS and its application. Chin Sci Bull, 2010, 55: 3545–3549
27 Tian L F, Yi S H, Zhao Y X, et al. Aero-optical wavefront measurement technique based on BOS and its applications. Chin Sci Bull, 2011, 56: 2320–2326
28 Zhao Y X, Tian L F, Yi S H. Supersonic flow imaging via nanoparticles. Sci China Ser E-Tech Sci, 2009, 52: 3640–3648
29 Fan J C. Modern Flow Visualization. Beijing: National Defense Industry Press, 2002. 145–147